Journal of Alloys and Compounds 505 (2010) 29–33

Contents lists available at ScienceDirect

Journal of Alloys and Compounds

journal homepage: www.elsevier.com/locate/jallcom

Magnetic properties of Mn-rich Pd_2MnSn Heusler alloys

T. Kanomata[a,*], K. Endo[a], Y. Chieda[a], T. Sugawara[a], K. Obara[b], T. Shishido[b], K. Matsubayashi[c], Y. Uwatoko[c], H. Nishihara[d], R.Y. Umetsu[b], M. Nagasako[e], R. Kainuma[e]

[a] Faculty of Engineering, Tohoku Gakuin University, Tagajo 985-8537, Japan
[b] Institute for Materials Research, Tohoku University, Sendai 980-8577, Japan
[c] Institute for Solid State Physics, the University of Tokyo, Kashiwa 277-8581, Japan
[d] Faculty of Science and Technology, Ryukoku University, Otsu 520-2194, Japan
[e] Department of Materials Science, Tohoku University, Sendai 980-8579, Japan

ARTICLE INFO

Article history:
Received 28 April 2010
Received in revised form 26 May 2010
Accepted 28 May 2010
Available online 18 June 2010

Keywords:
Heusler alloy
Magnetic moment
Exchange interaction
Curie temperature
Pressure effect

ABSTRACT

$Pd_2Mn_{1+x}Sn_{1-x}$ ($0 \le x \le 0.30$) alloys crystallize in the cubic $L2_1$ structure. The lattice parameter a decreases linearly with increasing Mn concentration x. X-ray powder diffraction patterns indicate that the excess Mn atoms occupy the vacant Sn sites. All alloys exhibit the ferromagnetic behavior. The pressure change of the magnetic moment per formula unit at 5 K for Pd_2MnSn is independent of pressure. The Curie temperature of $Pd_2Mn_{1+x}Sn_{1-x}$ ($0 \le x \le 0.30$) alloys increases linearly with increasing x. Magnetization measurements make clear that the magnetic moment of Mn atoms, which substitute for Sn sites, is coupled antiferromagnetically to the magnetic moment of Mn atoms on the ferromagnetic Mn sublattice.

1. Introduction

Heusler alloys are usually defined as ternary ordered alloys formed at the stoichiometric composition X_2YZ with the $L2_1$ structure where X is any element which belongs to the end of the 3d, 4d or 5d series, Y is a 3d, 4d and 5d elements, while Z is an sp element. The $L2_1$ unit cell shown in Fig. 1 is comprised of four interpenetrating fcc sublattices A, B, C and D with origin (0 0 0), (1/4,1/4,1/4), (1/2,1/2,1/2) and (3/4,3/4,3/4), respectively.

Ferromagnetic shape memory alloys (FSMAs) with the $L2_1$ structure have attracted much attention due to their potential application as smart materials [1,2]. They show a large magnetic field-induced strain by the rearrangement of twin variants in the martensite phase [3]. Unlike the case of conventional shape memory alloys, the speed of shape change is not limited in this mechanism. Until now, several candidates for FSMAs have been reported. Among them, the stoichiometric Heusler alloy Ni_2MnGa was mostly studied [4,5]. Enkovaara et al. reported the magnetic ordering of $Ni_2Mn_{1+x}Ga_{1-x}$ ($-0.05 \le x \le 0.31$) alloys on the basis of both experiments and theory [6]. The total magnetic moment per formula unit, μ_s, of $Ni_2Mn_{1+x}Ga_{1-x}$ ($-0.05 \le x \le 0.31$) alloys has a maximum near the stoichiometric composition and it decreases linearly with increasing Mn concentration x in the composition range with $0 \le x \le 0.31$. They showed that the magnetic moments of excess Mn atoms are antiferromagnetically aligned to the other moments by first-principles calculations within the density-functional theory, which explained the concentration dependence of μ_s for $Ni_2Mn_{1+x}Ga_{1-x}$ ($0 \le x \le 0.31$) alloys.

Recently, $Ni_2Mn_{1+x}Sn_{1-x}$ alloys with the $L2_1$ structure have also attracted much attention due to their potential application as smart materials because $Ni_2Mn_{1+x}Sn_{1-x}$ alloys with $0.4 \lesssim x \lesssim 0.6$ undergo a martensite transition from the high temperature $L2_1$ structure to the low temperature orthorhombic structure [7]. Furthermore, $Ni_2Mn_{1+x}Sn_{1-x}$ alloys showed a magnetic field-induced reverse martensitic transition from a paramagnetic martensite phase to a ferromagnetic austenite phase [8–11]. This alloy system opens up to the possibility of utilizing the magnetic field-induced shape memory effect. More recently, we investigated the magnetic properties for $Ni_2Mn_{1+x}In_{1-x}$ ($0 \le x \le 0.32$) alloys with the $L2_1$ structure [12]. For $Ni_2Mn_{1+x}In_{1-x}$ ($0 \le x \le 0.32$) alloys, the magnetic moments of excess Mn atoms are ferromagnetically coupled to the other moments. Thus, the concentration dependencies of μ_s for $Ni_2Mn_{1+x}In_{1-x}$ ($0 \le x \le 0.32$) alloys and $Ni_2Mn_{1+x}Ga_{1-x}$ ($0 \le x \le 0.31$) alloys show different behavior.

In this paper we report the concentration dependence of μ_s for $Pd_2Mn_{1+x}Sn_{1-x}$ ($0 \le x \le 0.30$) alloys. Furthermore, we investigated the pressure change of the magnetic moment for Pd_2MnSn.

* Corresponding author. Tel.: +81 22 368 7249; fax: +81 22 368 7070.
E-mail address: kanomata@tjcc.tohoku-gakuin.ac.jp (T. Kanomata).

0925-8388/$ – see front matter © 2010 Elsevier B.V. All rights reserved.
doi:10.1016/j.jallcom.2010.05.176

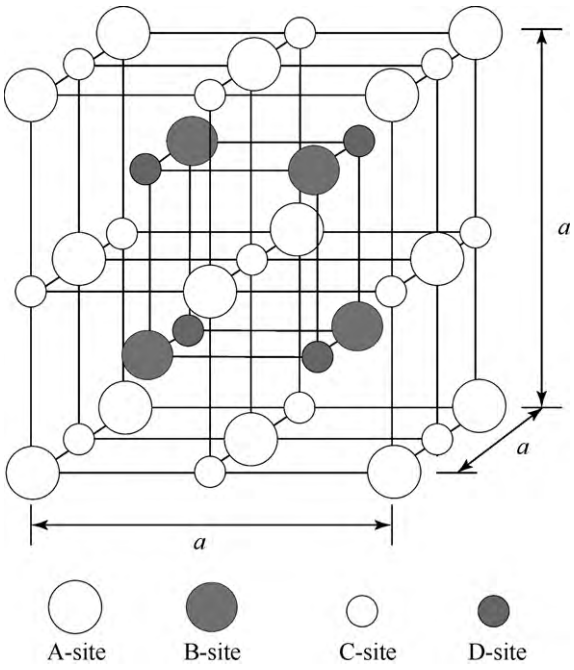

Fig. 1. Crystal structure of the Heusler-type alloy.

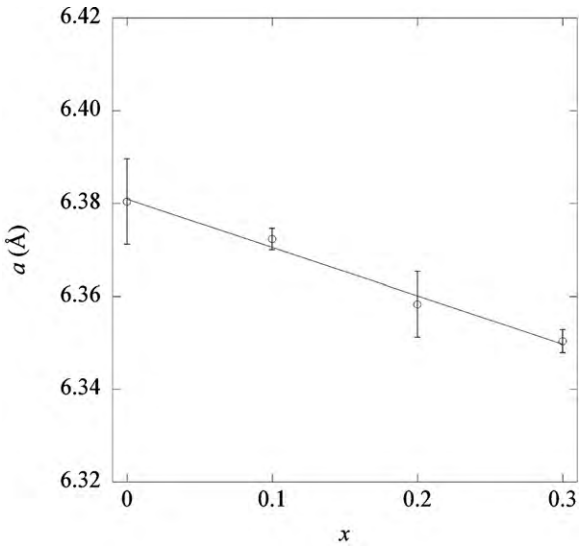

Fig. 2. Lattice parameter a versus concentration x for $Pd_2Mn_{1+x}Sn_{1-x}$ ($0 \le x \le 0.30$) alloys at room temperature. Solid line in the figure is a guide for the eyes.

2. Experimental

The polycrystalline $Pd_2Mn_{1+x}Sn_{1-x}$ ($0 \le x \le 0.30$) alloys were prepared by repeated arc melting of the appropriate quantities of the constituent elements, namely 99.9% pure Pd, 99.99% pure Mn and 99.999% pure Sn, in an argon atmosphere. Subsequently, samples were sealed in evacuated double silica tubes, heated at 850 °C for 3 days and then quenched in water. The phase characterization of the samples was carried out by X-ray powder diffraction measurements using Cu-Kα radiation.

The Curie temperature T_C was determined by an ac transformer method. The primary and secondary coils were wound on the sample rod with about 1 mm in diameter. An ac current with a constant amplitude flowed in the primary coil and the secondary voltage, which is directly proportional to the initial permeability, was recorded as a function of temperature. The frequency of the ac magnetic field is 1 kHz. The temperature was measured with a chromel–alumel thermocouple, kept in contact with the sample.

Magnetization measurements at high pressure up to 10 kbar were performed using a superconducting quantum interference device (SQUID) magnetometer and a piston-cylinder-type pressure cell made by CuBe alloy. The applied pressure was estimated from the superconducting critical temperature using a tin manometer. The sample and the tin manometer were compressed in a Teflon capsule filled with a liquid pressure-transmitting medium (Daphne 7373). The magnetization M_{cell} arising from the pressure cell with the Teflon capsule, the pressure-transmitting medium and tin manometer was estimated from the difference between the magnetization at 5 K with and without the pressure cell. All the magnetization data were collected by subtracting M_{cell}.

3. Results and discussions

For $Pd_2Mn_{1+x}Sn_{1-x}$, alloys, samples with $0 \le x \le 0.30$ are shown to crystallize in the cubic structure at room temperature by X-ray powder diffraction measurements. Fig. 2 shows the concentration dependence of the lattice parameter a at room temperature of $Pd_2Mn_{1+x}Sn_{1-x}$ ($0 \le x \le 0.30$) alloys. The lattice parameter decreases linearly with increasing the concentration x, which may be attributed to the difference in the atomic radii of Mn and Sn atoms. Recently, we observed a similar concentration dependence of the lattice parameter in $Ni_2Mn_{1+x}Sn_{1-x}$ ($0 \le x \le 0.46$) alloys and $Ni_2Mn_{1+x}In_{1-x}$ ($0 \le x \le 0.40$) alloys with the $L2_1$ crystal structure [12,13]. Fig. 3 shows the experimental and calculated X-ray powder diffraction patterns at room temperature for $Pd_2Mn_{1.3}Sn_{0.7}$. The profile refinement of the diffracted intensities using the standard Rietveld technique made clear that the specimen had the cubic $L2_1$ structure, in which A and C sites are occupied by Pd atoms, B and D sites occupied by Mn, and Sn and Mn atoms, respectively. Here we assumed that Sn and Mn atoms occupy the D site randomly. The goodness-of-fit indicator S is estimated to be 2.19. The good agreement between experimental and calculated X-ray powder diffraction patterns for $Pd_2Mn_{1.3}Sn_{0.7}$ shows that the $L2_1$ structure is a good representation of the actual structure, indicating that the excess Mn atoms in $Pd_2Mn_{1+x}Sn_{1-x}$ ($0 < x \le 0.30$) alloys preferentially occupy the vacant Sn site (D site). High-resolution powder neutron diffraction measurements on the magnetic shape memory alloy $Ni_2Mn_{1.44}Sn_{0.56}$ also made clear that the excess Mn atoms preferentially occupy the vacant Sn site [14].

We measured the temperature dependence of the initial permeability μ and the magnetization M at $H = 1$ kOe for $Pd_2Mn_{1+x}Sn_{1-x}$ ($0 \le x \le 0.30$) alloys. The inset in Fig. 4 shows the μ versus T curve for Pd_2MnSn. As shown in the figure, μ decreases rapidly just below T_C and takes a nearly constant value with further rise in tempera-

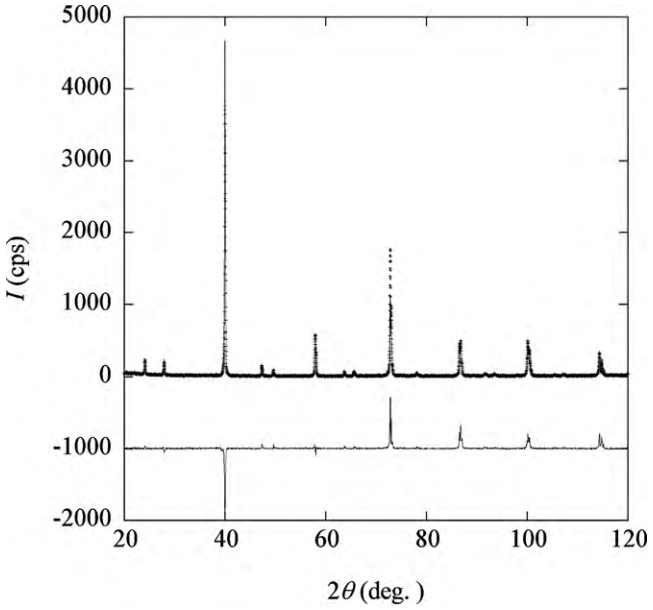

Fig. 3. The observed and calculated X-ray powder diffraction patterns at room temperature of $Pd_2Mn_{1.3}Sn_{0.7}$, together with the difference pattern.

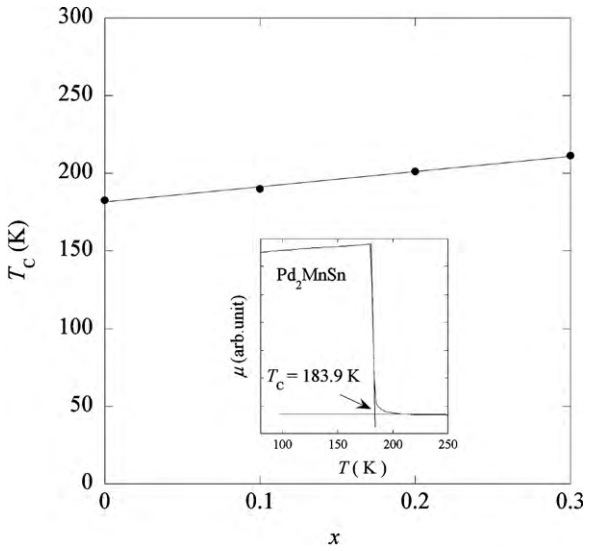

Fig. 4. Concentration dependence of the Curie temperature T_C for $Pd_2Mn_{1+x}Sn_{1-x}$ ($0 \le x \le 0.30$) alloys. The inset shows the initial permeability μ versus T curve for Pd_2MnSn.

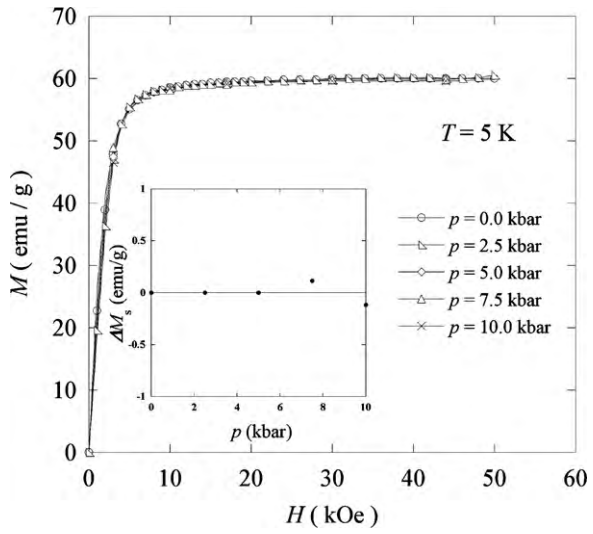

Fig. 6. Magnetization curves at 5 K of Pd_2MnSn at various pressures. The inset shows the ΔM_s versus p curve, where ΔM_s means the pressure change of the spontaneous magnetization M_s.

ture. The Curie temperature was defined as the cross point of linear extrapolation lines from both higher and lower temperature ranges on the μ versus T curve. The value of T_C for Pd_2MnSn is found to be 183.9 K, which is somewhat lower than those reported earlier [15–18]. Similar μ versus T curves were observed for samples with $0 < x \le 0.30$. Fig. 4 shows the concentration dependence of T_C for $Pd_2Mn_{1+x}Sn_{1-x}$ ($0 \le x \le 0.30$) alloys. No samples exhibited the martensitic transition in the temperature range from 5 K to 300 K. The Curie temperature increases linearly with increasing x.

Fig. 5 shows the temperature dependence of the magnetization M at H = 1 kOe for Pd_2MnSn. In a zero-field-cooled process (ZFC), a sample was first cooled to 5 K from room temperature under zero magnetic field; at this temperature the magnetic field H (=1 kOe) was applied and the magnetization was measured at this constant field with increasing temperature up to 375 K. Then, without removing the external field, the magnetization measurement was made with decreasing temperature, i.e., field-cooled (FC). The behavior of $M(T)$ for Pd_2MnSn is that of a typical ferromagnet. Even

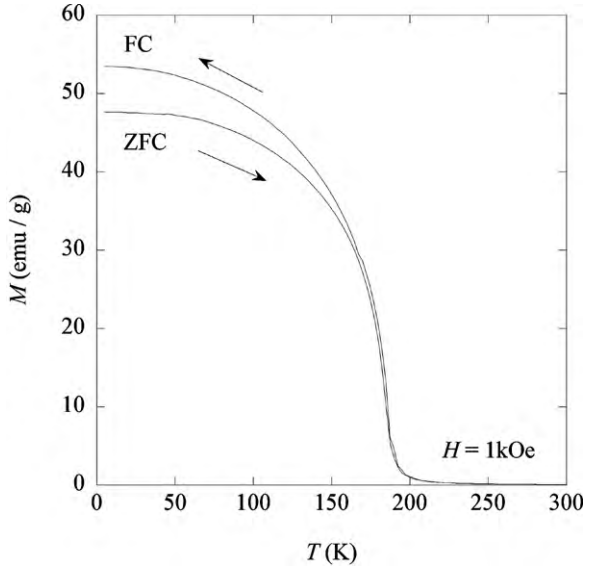

Fig. 5. Temperature dependence of the magnetization M at 1 kOe for Pd_2MnSn.

in the external magnetic field of 1 kOe, the splitting of the ZFC and FC curves appears as shown in Fig. 5. This may be attributed to the pinning effect of the domain wall.

Fig. 6 shows the magnetization curves at 5 K of Pd_2MnSn at various pressures. The spontaneous magnetization M_s under each pressure was determined by making an Arrott plot analysis. The inset in Fig. 6 shows the pressure dependence of ΔM_s for Pd_2MnSn, where ΔM_s is the pressure change of M_s. As shown in the inset, the magnetization is almost independent of pressure, indicating that Pd_2MnSn is the typical localized electron magnet. Shirakawa et al. investigated the pressure change of T_C for Pd_2MnSn [19]. According to their results, T_C increased linearly with increasing pressure. The value of dT_C/dp was found to be 0.76 K/kbar. Similar positive pressure dependences of T_C were observed for the ferromagnetic Heusler alloys $Cu_2Mn_{1.2}In_{0.8}$, Ni_2MnZ (Z = Al, Ga, Sn, Sb), Au_2MnAl, Pd_2MnSb and Rh_2MnZ (Z = Sn, Ge) [20–30]. The variation of the Curie temperature with pressure is caused by those of the exchange interaction and magnetization. In Pd_2MnSn the pressure dependence of the magnetization is nearly zero as shown in the inset in Fig. 6. So, only the variation of the exchange interaction should be taken into account. Kanomata et al. suggested a generalization of the interaction curve for the Mn-based Heusler alloys [23]. The available experimental values of the pressure derivative for the Mn-based Heusler alloys are consistent with those expected from the interaction curve proposed by Kanomata et al. [23].

The magnetization curves at 5 K under ambient pressure for $Pd_2Mn_{1+x}Sn_{1-x}$ ($0 \le x \le 0.30$) alloys are shown in Fig. 7. All of the magnetization curves are characteristic of ferromagnetism. The magnetization M at 5 K for all samples is saturated in a field of about 10 kOe, indicating that the magnetic crystalline anisotropy energy of $Pd_2Mn_{1+x}Sn_{1-x}$ ($0 \le x \le 0.30$) alloys is small. The spontaneous magnetization M_s at 5 K for $Pd_2Mn_{1+x}Sn_{1-x}$ ($0 \le x \le 0.30$) alloys was determined by an Arrott plot analysis. The magnetic moment per formula unit, μ_s, at 5 K for $Pd_2Mn_{1+x}Sn_{1-x}$ ($0 \le x \le 0.30$) alloys was estimated from the value of M_s and is plotted against x as shown in Fig. 8. The magnetic moment at 5 K of Pd_2MnSn was found to be $4.2\mu_B$/f.u. This value is in good agreement with those reported earlier [15,16]. Ishikawa et al. [31] and Khoi et al. [32] reported a somewhat smaller value of μ_s compared with that estimated in this study for Pd_2MnSn. It should be noted that the value of μ_s for Pd_2MnSn in this study is in good agreement with that calculated by Şaşıoğlu et al. [33]. As shown in Fig. 8,

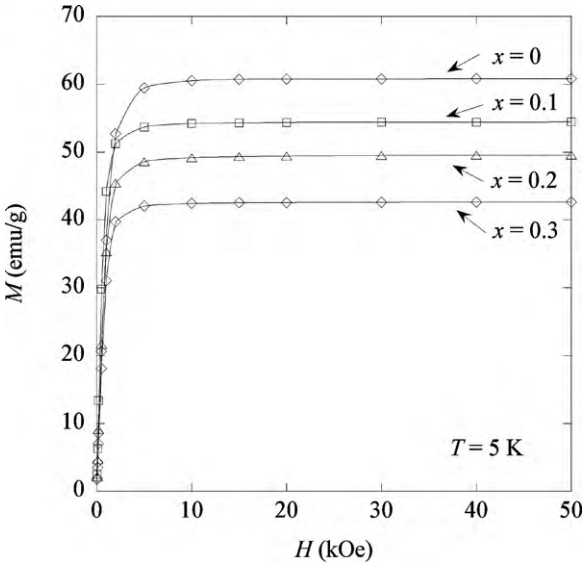

Fig. 7. Magnetization curves at 5 K for $Pd_2Mn_{1+x}Sn_{1-x}$ ($0 \le x \le 0.30$) alloys with various concentration x.

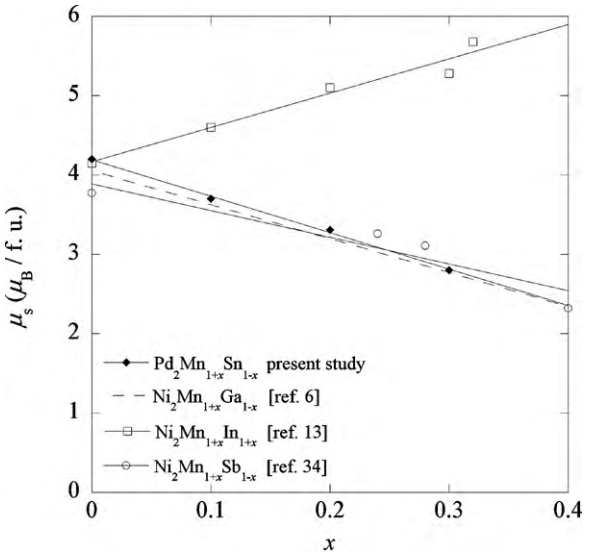

Fig. 9. The concentration dependence of the magnetic moment per formula unit, μ_s, at 4.2 K or 5 K for $Pd_2Mn_{1+x}Sn_{1-x}$ ($0 \le x \le 0.3$) alloys and $Ni_2Mn_{1+x}Z_{1-x}$ (Z = Ga, In, Sb) alloys. Solid lines in the figure are a guide for the eyes.

the experimental data show that the magnetic moment at 5 K of $Pd_2Mn_{1+x}Sn_{1-x}$ ($0 \le x \le 0.30$) alloys decreases linearly with increasing x. In order to explain the concentration dependence of the magnetic moment and to gain insight into the magnetic structure of the samples with $x \le 0.30$, we present a simple model. We assume that the magnetic moment of the Mn atoms substituted onto Sn sites in $Pd_2Mn_{1+x}Sn_{1-x}$ ($0 \le x \le 0.30$) alloys is antiferromagnetically coupled to the magnetic moment of the Mn atoms on Mn sites, and that the Mn magnetic moment μ_{Mn} on both sites is $4.08\mu_B$ and it remains constant with increasing x. Furthermore, we assume that the magnetic moments of Pd and Sn atoms, μ_{Pd} and μ_{Sn}, in $Pd_2Mn_{1+x}Sn_{1-x}$ ($0 \le x \le 0.30$) alloys are $0.08\mu_B$ and $-0.06\mu_B$, respectively and that they are independent of x. These values are Pd, Mn and Sn magnetic moments for Pd_2MnSn calculated by Şaşıoğlu et al. [33]. Then, μ_s (cal) of $Pd_2Mn_{1+x}Sn_{1-x}$ ($0 \le x \le 0.30$) alloys is given by $\mu_s(\text{cal}) = 2\mu_{Pd} + (1-x)\mu_{Mn} + (1-x)\mu_{Sn}$ μ_B. The solid line in Fig. 8 is the curve calculated using the above equation. As seen in Fig. 8, the experimental values of the samples with $x \le 0.3$ are in good agreement with the calculated ones. Fig. 9 shows the concentration dependence of μ_s at 4.2 K or 5 K for $Pd_2Mn_{1+x}Sn_{1-x}$ ($0 \le x \le 0.30$) alloys and Mn-rich Ni_2MnZ (Z = Ga, In, Sb) alloys. As shown in Fig. 9, the concentration dependence of μ_s for $Ni_2Mn_{1+x}Ga_{1-x}$ alloys [6] and $Ni_2Mn_{1+x}Sb_{1-x}$ alloys [34] show a similar behavior to that of $Pd_2Mn_{1+x}Sn_{1-x}$ alloys in this study. On the other hand, μ_s at 5 K of $Ni_2Mn_{1+x}In_{1-x}$ alloys increases linearly with increasing x. Khoi et al. studied the hyperfine fields and magnetic interactions in off-stoichiometric Ni_2MnSn and Pd_2MnSn using NMR spin echo method [35]. They estimated the nearest neighbor Mn–Mn exchange interaction J_0 between the magnetic moment of Mn atoms on Sn sites and the magnetic moment of Mn atoms on Mn sites using the molecular field approximation. According to their analysis, the exchange interaction parameter J_0, which appears only in the off-stoichiometric Ni_2MnSn and Pd_2MnSn, have very large and negative values. More recently, Chieda et al. showed from the pressure effect of T_C that the absolute value of J_0 for $Ni_2Mn_{1+x}Sn_{1-x}$ ($0.0 \le x \le 0.28$) alloys decreases steeply with increasing pressure [30]. The antiferromagnetic coupling between the magnetic moment of Mn atoms on Sn sites and the magnetic moment of Mn atoms on Mn sites for the Mn-rich Pd_2MnSn found in this study is consistent with the results of NMR measurements by Khoi et al. [35]. Recently, Şaşıoğlu et al. investigated the exchange mechanism in various Mn-based semi- and full-Heusler alloys containing Ni_2MnSn and Pd_2MnSn using the augmented spherical wave method within the atomic-sphere approximation [33]. They showed that the magnetic behavior of the Mn-based semi- and full-Heusler alloys depends on the competition of a Ruderman–Kittel–Kasuya–Yoshida (RKKY)-type ferromagnetic interaction and an antiferromagnetic superexchange interaction. For the stoichiometric Mn-based Heusler alloys, the direct coupling does not play a substantial role and can be ignored [36]. In the case of the coupling between the magnetic moment of Mn atoms on Sn sites and the magnetic moment of Mn atoms on Mn sites for the Mn-rich Pd_2MnSn alloys, the direct coupling may play a substantial role because the nearest neighbor Mn-Mn distance is about 3.2 Å, which is much smaller compared with the second nearest neighbor Mn–Mn distance in the Mn-rich Pd_2MnSn alloys. It should be noted that the second nearest neighbor Mn–Mn distance in the Mn-rich Pd_2MnSn alloys corresponds to the nearest neighbor Mn–Mn

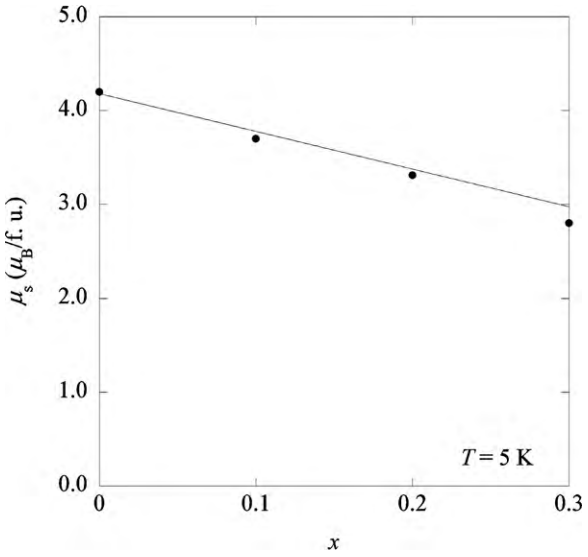

Fig. 8. Concentration dependence of the magnetic moment per formula unit, μ_s, at 5 K for $Pd_2Mn_{1+x}Sn_{1-x}$ ($0 \le x \le 0.30$) alloys. The solid line in the figure is the curve calculated using the model indicated in the text.

distance in the stoichiometric Mn-based Heusler alloys. Thus, the antiferromagnetic coupling between the magnetic moment of Mn atoms on Sn sites and the magnetic moment of Mn atoms on Mn sites in the Mn-rich Pd_2MnSn alloys may be attributed to the competition of the direct, the superexchange and the RKKY interactions. As far as we know, very little is known theoretically about the magnetic coupling between the magnetic moment of Mn atoms on Mn sites, and the magnetic moment of Mn atoms on Z (Z = Ga, In, Sb) sites for the Mn-rich Ni_2MnZ alloys and on Sn sites for the Mn-rich Pd_2MnSn alloys except for the discussion in Ref. [6].

4. Conclusions

$Pd_2Mn_{1+x}Sn_{1-x}$ ($0 \le x \le 0.30$) alloys crystallize in the $L2_1$ structure. The lattice parameter a at room temperature decreases linearly with increasing x. The structural refinements of $Pd_2Mn_{1+x}Sn_{1-x}$ ($0 \le x \le 0.30$) alloys were performed by X-ray powder diffraction data using the standard Rietveld technique. We confirmed that the excess Mn atoms on $Pd_2Mn_{1+x}Sn_{1-x}$ ($0 < x \le 0.30$) alloys occupy the vacant Sn sites. The Curie temperature increases with increasing x. This experiment proved that the magnetic moment of Mn atoms substituted onto Sn sites in $Pd_2Mn_{1+x}Sn_{1-x}$ ($0 < x \le 0.30$) alloys is antiferromagnetically coupled to the magnetic moment of Mn atoms on Mn sites. The magnetic moment per formula unit at 5 K of Pd_2MnSn is almost independent of pressure.

Acknowledgements

This work was partly supported by a grant based on the High-Tech Research Center Program for private universities from the Japan Ministry of Education, Culture, Sports, Science and Technology and in part it was supported by a Grant-in-Aid for Scientific Research (No. 21560693) from the Japan Society for the Promotion of Science. This work was partly carried out by the joint research in the Institute for Solid State Physics, the University of Tokyo.

References

[1] A. Planes, L. Mańosa, A. Saxena (Eds.), Magnetism and Structure in Functional Materials, Springer Verlag, Berlin, 2005.
[2] V.A. Chernenko (Ed.), Advances in Shape Memory Materials, Trans Tch Publications, Switzerland, 2008.
[3] K. Ullakko, J.K. Huang, C. Kantner, R.C. O'Handley, V.V. Kokorin, Appl. Phys. Lett. 69 (1996) 1966.
[4] P.J. Brown, J. Crangle, T. Kanomata, M. Matsumoto, K.-U. Neumann, B. Ouladdiaf, K.R.A. Ziebeck, J. Phys.: Condens. Matter 14 (2002) 10159.
[5] P. Entel, V.D. Buchelnikov, V.V. Khovailo, A.T. Zayak, W.A. Adeagbo, M.E. Gruner, H.C. Herper, E.F. Wassermann, J. Phys. D: Appl. Phys. 39 (2006) 865.
[6] J. Enkovaara, O. Heczko, A. Ayuela, R.M. Nieminen, Phys. Rev. B 67 (2003) 212405.
[7] Y. Sutou, Y. Imano, N. Koeda, T. Omori, R. Kainuma, K. Ishida, K. Oikawa, Appl. Phys. Lett. 85 (2004) 4358.
[8] R. Kainuma, Y. Imano, W. Ito, H. Morito, Y. Sutou, K. Oikawa, A. Fujita, K. Ishida, S. Okamoto, O. Kitakami, T. Kanomata, Appl. Phys. Lett. 88 (2006) 192513.
[9] R. Kainuma, K. Oikawa, W. Ito, Y. Sutou, T. Kanomata, K. Ishida, J. Mater. Chem. 18 (2008) 1837.
[10] D.L. Schlagel, W.M. Yuhasz, K.W. Dennis, R.W. McCallum, T.A. Lograsso, Scripta Mater. 59 (2008) 1083.
[11] R.Y. Umetsu, R. Kainuma, Y. Amako, Y. Taniguchi, T. Kanomata, K. Fukushima, A. Fujita, K. Oikawa, K. Ishida, Appl. Phys. Lett. 93 (2008) 042509.
[12] T. Kanomata, K. Fukushima, H. Nishihara, R. Kainuma, W. Ito, K. Oikawa, K. Ishida, K.-U. Neumann, K.R.A. Ziebeck, Mater. Sci. Forum 583 (2008) 119.
[13] T. Kanomata, T. Yasuda, S. Sasaki, H. Nishihara, R. Kainuma, W. Ito, K. Oikawa, K. Ishida, K.-U. Neumann, K.R.A. Ziebeck, J. Magn. Magn. Mater. 321 (2009) 773.
[14] P.J. Brown, A.P. Gandy, K. Ishida, R. Kainuma, T. Kanomata, K.-U. Neumann, K. Oikawa, B. Ouladdiaf, K.R.A. Ziebeck, J. Phys.: Condens. Matter 18 (2006) 2249.
[15] P.J. Webster, R.S. Tebble, Phil. Mag. 16 (1967) 347.
[16] P.J. Webster, M.R.I. Ramadan, J. Magn. Magn. Mater. 5 (1977) 51.
[17] G.L.F. Fraga, D.E. Brandáo, J. Magn. Magn. Mater. 102 (1991) 199.
[18] G.L.F. Fraga, L.A. Borba, P. Pureur, Phys. Rev. B 74 (2006) 064427.
[19] K. Shirakawa, T. Kanomata, T. Kaneko, J. Magn. Magn. Mater. 70 (1987) 421.
[20] T. Hirone, T. Kaneko, K. Kondo, J. Phys. Soc. Japan 18 (1963) 65.
[21] I.G. Austin, P.K. Mishra, Phil. Mag. 15 (1967) 529.
[22] T. Kaneko, H. Yoshida, S. Abe, K. Kamigaki, J. Appl. Phys. 52 (1981) 2046.
[23] T. Kanomata, K. Shirakawa, T. Kaneko, J. Magn. Magn. Mater. 65 (1987) 76.
[24] V.V. Kokorin, S.V. Cherepov, V.A. Chernenko, Phys. Met. Metall. 63 (1987) 177.
[25] V.V. Kokorin, I.A. Osipenko, T.V. Shirina, Phys. Met. Metall. 67 (1989) 173.
[26] A.G. Gavriliuk, G.N. Stepanov, V.A. Sidorov, S.M. Irkaev, J. Appl. Phys. 79 (1996) 2609.
[27] S. Kyuji, S. Endo, T. Kanomata, F. Ono, Physica B 237–238 (1997) 523.
[28] Y. Adachi, H. Morita, T. Kanomata, A. Sato, H. Yoshida, T. Kaneko, H. Nishihara, J. Alloys Compd. 383 (2004) 37.
[29] J. Kamarád, F. Albertini, Z. Arnold, F. Casoli, L. Pareti, A. Paoluzi, J. Magn. Magn. Mater. 290–291 (2005) 669.
[30] Y. Chieda, T. Kanomata, K. Fukushima, K. Matsubayashi, Y. Uwatoko, R. Kainuma, K. Oikawa, K. Ishida, K. Obara, T. Shishido, J. Alloys Compd. 486 (2009) 51.
[31] Y. Ishikawa, K. Tajima, P. Radhakrishna, J. Phys. Soc. Japan 40 (1976) 1597.
[32] L.D. Khoi, P. Veillet, J. Schaf, I.A. Campbell, J. Phys. F: Met. Phys. 12 (1982) 2055.
[33] E. Şaşıoğlu, L.M. Sandratskii, P. Bruno, Phys. Rev. B 77 (2008) 064417.
[34] M. Khan, I. Dubenko, S. Stadler, N. Ali, J. Phys.: Condens. Matter 20 (2008) 235204.
[35] L.D. Khoi, P. Veillet, I.A. Campbell, J. Phys. F: Met. Phys. 8 (1978) 1811.
[36] E. Şaşıoğlu, L.M. Sandratskii, P. Bruno, Phys. Rev. B 70 (2004) 024427.